

Award Number: DoD Award W81XWH-11-1-0189

TITLE: Novel Synergistic Therapy for Metastatic Breast Cancer: Magnetic Nanoparticle Hyperthermia of the Neovasculature Enhanced by a Vascular Disruption Agent

PRINCIPAL INVESTIGATOR: Natalie L. Adolphi, Ph.D.

CONTRACTING ORGANIZATION: University of New Mexico Health Sciences Center
Albuquerque, NM 87131-0001

REPORT DATE: April 2013

TYPE OF REPORT: Final

PREPARED FOR: U.S. Army Medical Research and Materiel Command
Fort Detrick, Maryland 21702-5012

DISTRIBUTION STATEMENT: Approved for Public Release;
Distribution Unlimited

The views, opinions and/or findings contained in this report are those of the author(s) and should not be construed as an official Department of the Army position, policy or decision unless so designated by other documentation.

REPORT DOCUMENTATION PAGE				Form Approved OMB No. 0704-0188	
Public reporting burden for this collection of information is estimated to average 1 hour per response, including the time for reviewing instructions, searching existing data sources, gathering and maintaining the data needed, and completing and reviewing this collection of information. Send comments regarding this burden estimate or any other aspect of this collection of information, including suggestions for reducing this burden to Department of Defense, Washington Headquarters Services, Directorate for Information Operations and Reports (0704-0188), 1215 Jefferson Davis Highway, Suite 1204, Arlington, VA 22202-4302. Respondents should be aware that notwithstanding any other provision of law, no person shall be subject to any penalty for failing to comply with a collection of information if it does not display a currently valid OMB control number. PLEASE DO NOT RETURN YOUR FORM TO THE ABOVE ADDRESS.					
1. REPORT DATE April , 2013		2. REPORT TYPE Final		3. DATES COVERED 1 June 2011 – 31 March 2013	
4. TITLE AND SUBTITLE Novel Synergistic Therapy for Metastatic Breast Cancer: Magnetic Nanoparticle Hyperthermia of the Neovasculature Enhanced by a Vascular Disruption Agent				5a. CONTRACT NUMBER	
				5b. GRANT NUMBER W81XWH-11-1-0189	
				5c. PROGRAM ELEMENT NUMBER	
6. AUTHOR(S) Natalie L. Adolphi, Ph.D. E-Mail: NAdolphi@salud.unm.edu				5d. PROJECT NUMBER	
				5e. TASK NUMBER	
				5f. WORK UNIT NUMBER	
7. PERFORMING ORGANIZATION NAME(S) AND ADDRESS(ES) University of New Mexico Health Sciences Center Albuquerque, NM 87131-0001				8. PERFORMING ORGANIZATION REPORT NUMBER	
9. SPONSORING / MONITORING AGENCY NAME(S) AND ADDRESS(ES) U.S. Army Medical Research and Materiel Command Fort Detrick, Maryland 21702-5012				10. SPONSOR/MONITOR'S ACRONYM(S)	
				11. SPONSOR/MONITOR'S REPORT NUMBER(S)	
12. DISTRIBUTION / AVAILABILITY STATEMENT Approved for Public Release; Distribution Unlimited					
13. SUPPLEMENTARY NOTES					
14. ABSTRACT Vascular disruption agents (VDAs) have been shown to selectively destroy established tumor vasculature, which results in the ischemic death of up to 99% of tumor cells. The weakness of VDA monotherapy is that it often leaves a rim of surviving tumor cells which can then regrow and spread. The overall goal of this study (addressed in Task 2) was to enhance VDA therapy by inducing hyperthermia, targeted to the neovascular endothelium, through the use of superparamagnetic iron oxide nanoparticles (SPIONs), in order to halt, or significantly slow down tumor growth. Therefore, the first aim of this study (Task 1) was to maximize the delivery of SPIONs to the tumor rim, through a combination of neovascular targeting and increased vascular permeability induced by the VDA. Covalent coupling of primary amines on VEGFR-2 antibodies to carboxyl groups on the SPIONs activated by EDC/Sulfo-NHS resulted in stable particles that showed specific binding to endothelial cells in vitro. Current in vivo results suggest a modest enhancement of SPION delivery to the tumor rim when αVEGFR-2 targeting of PEG-coated particles and 15 min pre-administration of DMXAA (a VDA) are employed. The results suggest that the combination of targeting the neovasculature and increasing vascular permeability through the action of the VDA is an effective SPION delivery strategy; however, statistically-significant nanoparticle quantitation (by mass spectrometry) was not realized, due to high endogenous iron levels in tumor tissue. In vitro testing of SPION heating in the presence of an alternating magnetic field demonstrated that heating is optimized using 20 nm SPIONs. Reformulation of the poorly soluble DMXAA (using bicarbonate buffer to replace DMSO) was shown to improve long-term survival of the mice after DMXAA administration, which will enable in vivo longitudinal measurements of therapeutic efficacy to be carried out in a future study.					
15. SUBJECT TERMS none provided					
16. SECURITY CLASSIFICATION OF:			17. LIMITATION OF ABSTRACT	18. NUMBER OF PAGES	19a. NAME OF RESPONSIBLE PERSON
a. REPORT	b. ABSTRACT	c. THIS PAGE			USAMRMC
U	U	U	UU		19b. TELEPHONE NUMBER (include area code)

Table of Contents

	<u>Page</u>
Introduction.....	4
Body.....	5
Key Research Accomplishments.....	19
Reportable Outcomes.....	19
Conclusion.....	20
References.....	21
Appendices.....	none

Novel Synergistic Therapy for Metastatic Breast Cancer: Magnetic Nanoparticle Hyperthermia of the Neovasculature Enhanced by a Vascular Disruption Agent

Introduction

Vascular disruption agents (VDAs) have been shown to selectively destroy established tumor vasculature, which results in the ischemic death of up to 99% of tumor cells^[1]. The weakness of this therapy alone is that it often leaves a rim of surviving tumor cells which can then regrow and spread^[1]. *The overall goal of this study (addressed in Task 2) is to enhance VDA therapy by inducing hyperthermia, targeted to the neovascular endothelium, through the use of superparamagnetic iron oxide nanoparticles (SPIONs), in order to halt, or significantly slow down tumor growth. Therefore, the first aim of this study (Task 1) is to maximize the delivery of SPIONs to the tumor rim, through a combination of targeting and increase vascular permeability induced by the VDA.*

Targeted therapy takes advantage of biomarkers that are characteristic of the tumor environment in order to selectively treat tumor cells^[2]. Angiogenesis, the process by which new blood vessels are formed, plays a crucial role in development, wound repair, and inflammation^[2]. This process is exploited in cancer, and is essential for tumor growth beyond the size of about 1-2 mm in diameter^[8]. The integrin receptor $\alpha\beta3$, which is over-expressed on the activated endothelium of tumor neovasculature, is a glycoprotein membrane receptor which recognizes ECM proteins expressing an arginine-glycine-aspartic acid (RGD) peptide sequence^[3,10]. The integrin receptor $\alpha\beta3$ is a strong potential anti-angiogenic target because it is up-regulated in both cancer cells and tumor associated blood vessels^[9]. Peptide ligands containing the RGD triad display both a strong affinity, as well as selectivity to the $\alpha\beta3$ integrin^[11,19]. However, in our work, SPIONs, when bound directly to the RGD containing peptide c(RGDfK), demonstrated poor specific binding when compared to controls. Though the conjugation was shown to be successful, these results could be due to mis-orientation of c(RGDfK) on the particle surface, or steric hinderance from SPIONs at the active site for $\alpha\beta3$ integrin. To target $\alpha\beta3$, SPIONs were first conjugated to a small molecule ligand, cyclic RGD, c(RGDfK).

Observed functional inactivity of the RGD-conjugated particles led to the replacement of the c(RGDfK) ligand with an antibody against vascular endothelial growth factor receptor 2 (α VEGFR-2). An antibody against VEGFR-2 was selected to replace the c(RGDfK) conjugate because of the role of VEGFR-2 over-activation in angiogenesis^[2]. VEGFR-2 is a receptor tyrosine kinase expressed primarily at the surface of endothelial cells, which is auto-phosphorylated through stimulation by circulating VEGF-A to induce endothelial proliferation^[4]. High levels of tumor VEGF-A production, shown to up-regulate VEGFR-2 gene expression, correlates with the over-expression of VEGFR-2 at the tumor vasculature^[4]. α VEGFR-2 targeted contrast agents have been shown to correlate with the relative expression of VEGFR-2 and the vascular phenotype of tumors in mouse models, demonstrating the effectiveness of this modality^[12].

The cross-reactivity of α VEGFR-2 in both mice and humans was also an important intention in our selection of the antibody clone, because the MDA-MB-231 xenograft tumor cells are human derived, whereas the host for the tumor is a NOD SCID mouse. Therefore the tumor will consist of human breast cancer cells, and the vasculature will consist of mouse endothelial cells. Thus a clone that reacts with both mouse and human VEGFR-2 was chosen. Further, the activity of α VEGFR-2 targeted SPIONs was tested in vitro on human umbilical vein endothelial cells (HUVEC), so the ability to use an antibody with a similar affinity for human and mouse VEGFR-2 simplified the determination of whether the SPION conjugation was successful. The functionalization of α VEGFR-2-conjugated SPIONs was successfully demonstrated by their specific association with the cell surface of human umbilical vein endothelial cells (HUVEC) when compared to a non-specific Immunoglobulin G (IgG)-conjugated SPION control.

In addition to targeting, we hypothesize that VDAs may co-facilitate SPION delivery to the tumor rim. The initial changes at the active tumor endothelium which are induced by VDAs include the reorganization of the cytoskeletal network and the alteration of the junctions between endothelial cells^[13]. This response is generally rapid (within 1 h), and results in the enhanced permeability of the endothelium^[13]. Downstream

effects triggered by VDAs further lead to the induction of tumor hemorrhagic necrosis[14], and the ischemic death of up to 99% of tumor cells[1]. In order to demonstrate the enhanced endothelial permeability effects on SPION delivery to tumors, subcutaneous xenograft breast tumor-bearing mice were first treated with DMXAA (5,6-dimethylxanthenone-4-acetic acid), a low-molecular-weight VDA. The delay between DMXAA administration and the injection of the α VEGFR-2 SPIONs that maximizes the SPION concentration in the viable tumor rim was determined by the time variable delivery (15 min, 30 min, or 60 min) of α VEGFR-2 conjugated SPIONs following VDA administration.

Our current results suggest that VDAs appear to enhance the delivery of α VEGFR-2-conjugated SPIONs to the tumor rim, by promoting increased permeability of neovascular endothelial cells^[4]. To demonstrate VDA enhanced delivery, NOD-SCID mice were induced with two subcutaneous xenograft MDA-MB-231 breast tumors. The first group of mice was treated with either α VEGFR-2-conjugated SPIONs, IgG-conjugated SPIONs, or unconjugated SPIONs (PEG only) both without VDA treatment. A second group is currently being assessed under time variable delivery of α VEGFR-2-conjugated SPIONs, IgG-conjugated SPIONs, or unconjugated SPIONs (PEG only) following VDA treatment. The effects of these treatments are observed qualitatively through Prussian blue histology in order to determine the conditions for maximum SPION delivery to the tumor rim. To quantify the nanoparticle delivery to tumors in vivo, we attempted to use chemical analysis (by inductively coupled plasma mass spectrometry, ICP-MS) to detect the iron delivered to the tumors in the form of SPIONs. Unfortunately, we found that while ICP-MS is sensitive enough to quantify the iron at levels appropriate to monitor nanoparticle delivery to tumors, the endogenous background levels of iron in breast tumor tissue are significant and variable; the variation observed in normal tissue was unfortunately greater than the quantity of iron to be delivered as nanoparticles.

Further changes in neovascular permeability in response to VDAs, which include the induction of endothelial apoptosis^[16], blood vessel rupture, and a boost of N_2O ^[17] are all reported to occur after about 12-24 h. We hypothesized that these late alterations in tumor physiology after VDA treatment may also be favorable to increasing SPION delivery. In the process of evaluating this hypothesis in vivo, we discovered that the tumor-bearing NOD/SCID mice were not surviving DMXAA pre-treatment for more than 6 hours. This led the development of a new bicarbonate formulation of the drug that was well-tolerated over many days. With the new DMXAA formulation, we then performed a number of experiments, including verification (using Hoechst staining) of the drug's ability to alter perfusion/permeability in tumors and tests of whether longer VDA pre-treatments (20 hours) increase SPION delivery to the tumor rim.

Having determined methods for increasing SPION delivery to tumors in this study, targeted hyperthermia will be induced in vivo in future studies by exposing the SPIONs to an alternating magnetic field (AMF). When exposed to an AMF, SPIONs generate heat as a result of hysteresis and relaxational losses, which results in the heating of tissue in which SPIONs accumulate[5]. We will also investigate whether the heating effect can be utilized to trigger release of additional chemotherapeutic from drug-loaded nanoparticles.

Body

Materials and Methods

SPION Surface Functionalization

The conjugation of c(RGDfK) peptide to 15 nm carboxyl functionalized SPIONs was performed using a covalent link with the amine group of the peptide and the carboxyl group of the SPIONs using the Ocean NanoTech Carboxyl Magnetic Iron Oxide Nanocrystals Conjugation Kit. First, 0.2 mL of SPIONs (5 mg Fe/mL) were activated by incubating with a molar ratio 2000:1 of sulfo-N-hydroxysuccinimide and 1-ethyl-3, 3-dimethylaminopropyl carbodiimide hydrochloride (EDAC) for 20 min in a borate buffered solution, pH 5.5, after which the pH was adjusted to 8.0. The protein (0.2 mg) was added immediately, mixed well, and incubated for 2 h at room temperature. The resulting nanocrystal conjugates were purified by centrifugation at 18350 RCF (12800 RPM) twice for 1 h each, and stored in 1 mL borate buffered solution, pH 7.4.

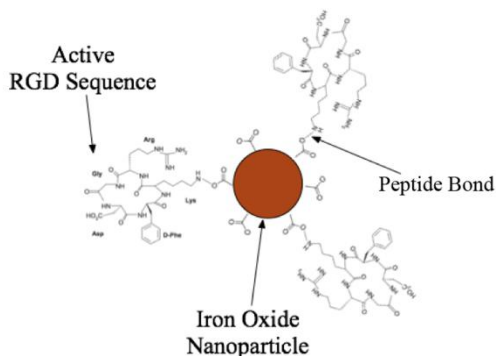
This method was repeated using 0.2 mg c(RADfK) peptide as a negative control. In order to separate the RGD binding sequence further from the particle surface as a way to overcome steric hinderance, this method was repeated for 0.2 mg c(RGDfK)(PEG-PEG)) peptide. This RGD analog contains two PEG derivatives (8-amino-3,6-dioxaoctanoic acids) that act as spacers between ligand and lipid head groups, to allow for more efficient binding[20]. For these experiments c(RADfK(PEG-PEG)) was conjugated by the same methods as a negative control.

For antibody conjugated SPIONs, these methods were repeated using 0.02 mg polyclonal α VEGFR-2. As a negative control, 0.02 mg of polyclonal normal mouse immunoglobulin G (IgG) was conjugated to SPIONs, also by the same methods.

In order to improve SPION circulation time for more effective tumor delivery in vivo, these methods were repeated for 0.02 mg polyclonal α VEGFR-2, as well as 0.02 mg IgG using particles which were functionalized with a PEG-Carboxyl coating. The polymeric PEG coating acts to further stabilize the particles, and has been shown to increase the blood half-life of particles in vivo by up to 5 fold [15].

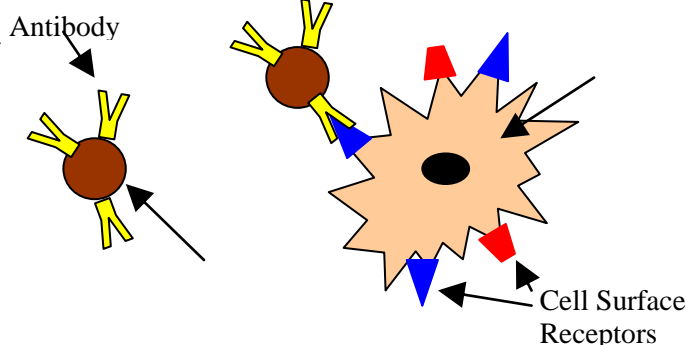
Figure 1:

A.



(A) Schematic illustration of a c(RGDfK)-conjugated SPION

B.



(B) Schematic illustration of antibody conjugated SPIONs interacting with cell surface receptors

Conjugated SPION Quantification

Stock 15 nm carboxyl functionalized SPIONs were diluted from a concentration of 5 mg Fe/mL to three individual cuvettes at 0.04 mg/mL, 0.02 mg/mL, and 0.01 mg/mL in di-H₂O. A full spectrum absorbance of each solution was generated using a Beckman Coulter DU 800 UV/Vis Spectrophotometer. To generate a standard curve, the absorbances at 350 nm for these particle solutions were plotted as a function of SPION concentration. Conjugated SPIONs (with unknown concentrations) were each diluted 1:500 in di-H₂O, and their concentrations were determined by plotting individual absorbances at 350 nm on the standard curve.

Because the carboxylic acid functional groups of SPIONs are strongly anionic when free, compared to when conjugated to protein, they freely form carboxylate salts with metal cations. If the surface charge is providing colloidal stabilization (i.e., the repulsion of like surface charges prevents the particles from aggregating), this shielding of the surface charge by ions can lead to aggregation and the precipitation of SPIONs in ionic solutions. To determine successful conjugation, 0.1 mg of SPIONs were mixed with 0.4 mL of serum free Dulbecco's Modified Eagle Medium:Nutrient Mixture F-12 (DMEM/F-12), which contains divalent cations for the purpose of cell culture. Visual inspection of the solution to look for particle stability was then compared 1 h after mixing in order to determine successful conjugation. Differences in this form of colloidal stability between un-conjugated and conjugated SPIONs imply that the surface modification was successful.

Cell Culture Conditions

HUVEC line was cultured at 37° C under a humidified atmosphere of 5% CO₂ and 95% air in MCDB-131 complete medium with fetal bovine serum and antibiotics (VEC Technologies) on gelatin coated surface. SK-OV-3 ovarian adenocarcinoma cell line was cultured at 37° C under a humidified atmosphere of 5% CO₂ and 95% air in McCoy's 5A medium supplemented with 10% fetal bovine serum (FBS), 1% glutamax, and 1% penicillin:streptomycin. MDA-MB-231 and MDA-MB-435 mammary gland adenocarcinoma cell lines were cultured at 37° C under a humidified atmosphere of 5% CO₂ and 95% air in DMEM/F-12 supplemented with 10% fetal bovine serum (FBS), 1% glutamax, and 1% penicillin:streptomycin.

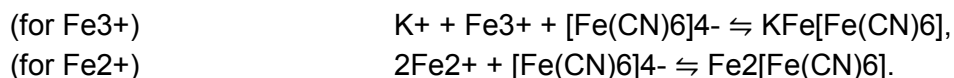
Conjugated SPION Cell Targeting

Cultured cells were divided into 4x6 well plates over poly-L-lysine coated cover slips at a concentration of 1×10^5 cells per well, and cultured overnight. The optimum SPION concentration for short-term cell targeting in culture was determined by preparing 2.5 mM incremental solutions within the range of 0 mM to 15 mM of c(RGDfK) conjugated SPIONs in serum free DMEM/F-12 media. Time dependence for the receptor mediated endocytosis of particles was then determined by incubating cultured cells with each solution in 15 min increments up to an hour at 37° C. All SPION incubations which followed were carried out with a 10mM solution of conjugated SPIONs in serum free culture media for 30 min. Adherent cells were washed with PBS, and fixed using 4% paraformaldehyde (PFA) in PBS buffer solution for 15 min. Fixed cells were then washed twice with PBS.

These conditions were repeated for $\alpha V\beta 3$ targeting using c(RADfK) conjugated SPIONs as a control. Conditions were also repeated using c(RGDfK)(PEG-PEG) conjugated SPIONs and c(RADfK)(PEG-PEG) conjugated SPIONs as a negative control. Finally, for VEGFR-2 targeting, these conditions were repeated using α VEGFR-2 conjugated SPIONs and IgG conjugated SPIONs as a control.

SPION Staining

Prussian blue is produced by mineral acid hydrolysis to release ferric ions, which then form a dark blue precipitate in the presence of ferrocyanide ions by the following reactions[21]:



This staining method was performed on fixed cells by incubating with equal parts 10% potassium ferrocyanide and 20% hydrochloric acid for 20 min. Cells were washed 3 times with di-H₂O and counterstained with nuclear fast red for 5 min. Stained cells were washed again 2 times with di-H₂O and mounted using VECTASHIELD mounting medium with DAPI.

The presence of antibody conjugated SPIONs was also detected using a secondary, fluorescent antibody. This was performed by first incubating fixed cells with blocking serum (3% normal goat serum) for 30 min with continuous mixing. Cells were then washed twice with PBS and incubated with a 1:250 solution of secondary antibody (rabbit α mouse 488) in PBS for 30 min with continuous mixing. Labeled cells were washed with PBS and mounted using VECTASHIELD mounting medium with DAPI. For each secondary antibody labeled experiment, a negative control was used which did not receive particle or antibody treatment.

Conjugated SPION Murine Tumor Delivery

Female NOD-SCID mice were bred at the University of New Mexico Animal Resource Facility. All mouse procedures were performed according to a protocol approved by the University of New Mexico Health Sciences IACUC. Prior to injection, MDA-MB 231 cells were collected and suspended with 50% MatriGel in DMEM/F-12 media and kept on ice. Two million cells were injected into each of the inguinal mammary fat pads of the NOD-SCID mice at 6-8 weeks of age. Tumor development was monitored weekly until the outer diameter reached about 10 mm in size.

On the day of injection, a total of 0.250 mg of SPIONs were re-suspended in 0.1 ml PBS and given to mice retro-orbitally. Tumors were collected either 2 or 5 h following the injection. Tissues were then fixed in 4% paraformaldehyde in PBS buffer solution overnight, and embedded in paraffin for sections. Tissue sections were deparaffinized and hydrated to water, stained using Prussian blue histology, dehydrated, cleared in xylene, and mounted in Permount.

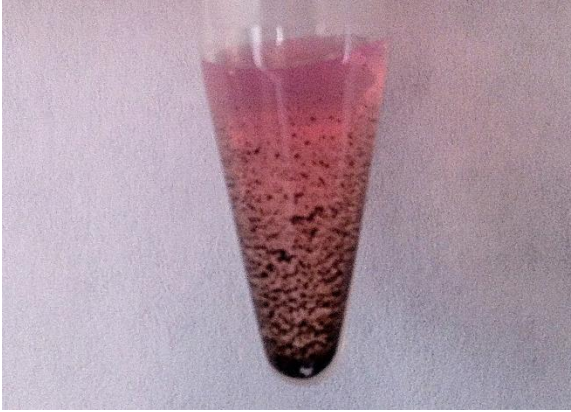
For VDA treated mice, DMXAA was dissolved in 10% DMSO/PBS and given to mice by intraperitoneal injection at a dose of 20 mg/kg, which is typical for other mouse studies[22]. However, this formulation was eventually shown to produce an adverse reaction (leading to pre-mature death) cause by the DMSO in tumor-bearing NOD/SCID mice. A new formulation was developed to eliminate the DMSO. DMXAA was dissolved in 5% sodium bicarbonate to produce a 10 mg/ml solution, then diluted 1:2 in 1x PBS to produce a 5 mg/ml solution, resulting in an approximately 100 microliter injection volume. The bicarbonate formulation produced no adverse reactions, but was shown to alter tumor vascular physiology in the desired manner (see results below).

Table 1. Mouse experiments performed. VDA was administered prior to SPION (or Hoechst Dye) delivery. The interval between VDA and SPION (or dye) administration is given in the column headings.

SPION prep	No VDA	15 m	30 m	60 m	2 h	3h	6 h	20 h
VEGFR-2	15	6	2			3		4
IgG	7	4				3		
PEG only (no Ab)	5	4	2					
PEG- carboxyl (no Ab)	1		2	2				
No SPIONs	3	1						
Hoechst Dye (no SPIONs)	3			1	5	2	2	2
Hoechst Dye (PEG SPIONs)	1	2				3		
Total Mice Studied:	85		Failed mouse experiments:	6			Total:	91

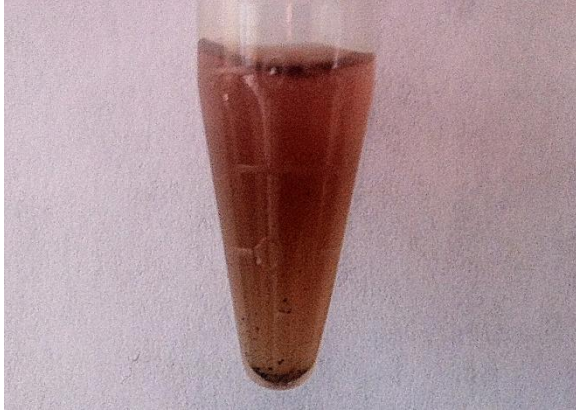
Figure 2:

A.



(A) Un-conjugated carboxyl-SPIONs in serum free DMEM/F-12 show significant aggregation after 1 h. Because the carboxylic acid functional groups of SPIONs are strongly anionic when un-conjugated to protein, they freely form carboxylate salts with metal cations. This shielding reduces repulsive electrostatic interactions and leads to the precipitation of un-conjugated SPIONs in culture media, which contains divalent cations for the purpose of cell culture.

B.



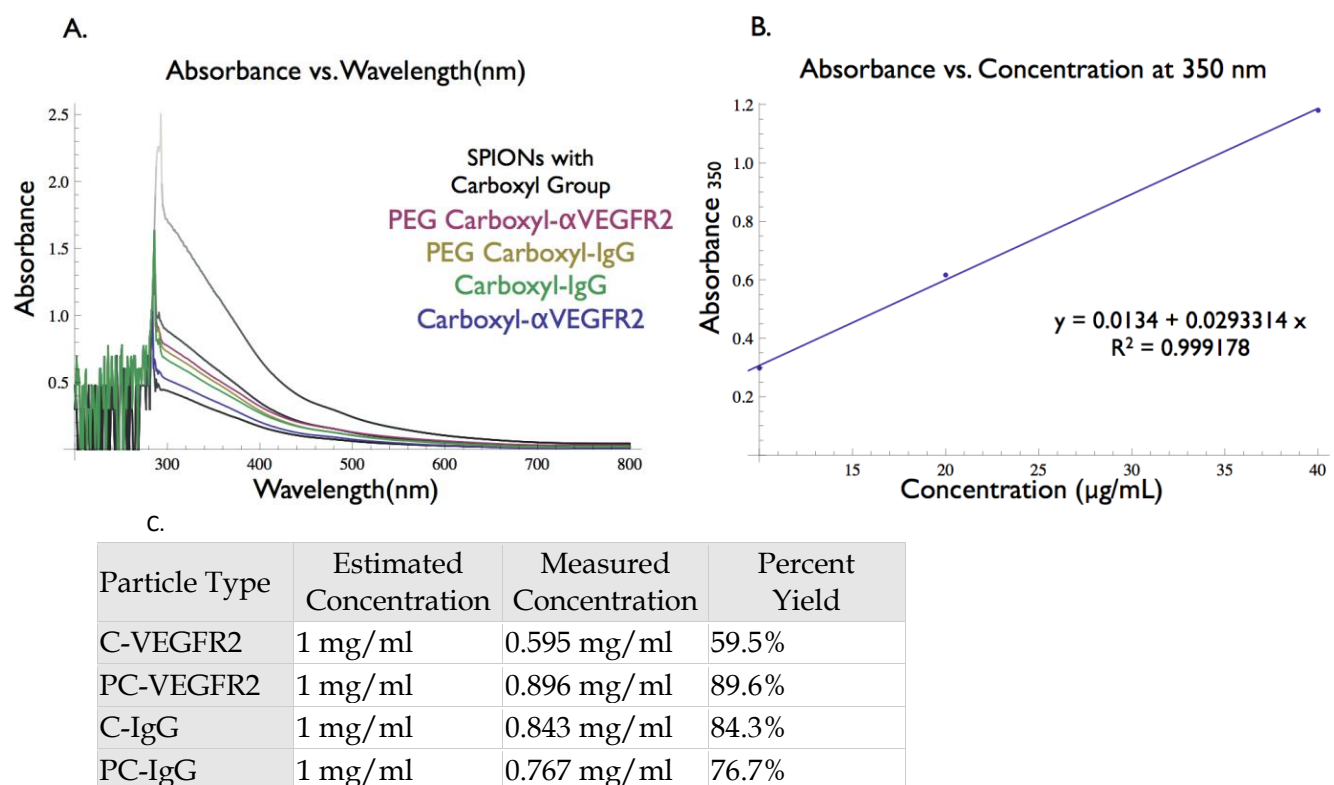
(B) α VEGFR-2 conjugated SPIONs in serum free DMEM/F-12 show reduced aggregation after 1 h. The peptide bond which is formed by the conjugation reaction replaces free carboxylic acid groups with a protein, which sterically stabilize the particles in solutions containing divalent cations. This result indicates that the SPION surface was successfully modified. This image is representative of each conjugation of antibody/peptide with carboxyl-SPIONs.

Results

SPION Surface Conjugation

A cross-linking reaction with carboxyl functionalized SPIONs using EDAC as an activating agent to couple the carboxyl groups on particles to amino-terminal groups on the antibody or peptides yielded particles with functional biocompatibility. Carboxyl-SPIONs conjugated with protein exhibited greater colloidal stability at biological pH, salinity, and temperature conditions compared to un-conjugated SPIONs, which formed a precipitate in culture medium (Figure 2). The addition of protein apparently provided steric stabilization, i.e. the protein provided a spacer that prevented particles from getting close enough together to aggregate due to attractive VanderWaals interactions. Because PEG-Carboxyl particles show native stability in biological pH, salinity, and temperature conditions prior to conjugation, no difference in solubility was observed following conjugation for PEG-Carboxyl particles. The PEG molecules provided steric stabilization, such that further addition of protein does not increase the stability. SPIONs conjugated with α VEGFR-2 antibody were effectively labeled with a secondary fluorescent antibody (rabbit α mouse 488). Furthermore, α VEGFR-2 conjugated showed a high level of binding to HUVECs (which express high levels of VEGFR-2) compared to an IgG conjugated SPION control, which showed a low level of binding (Figure 6). The absorbances of known concentrations of a standard (stock carboxyl-SPIONs) were measured at 350 nm, which was used to determine the concentrations of conjugated SPION solutions (Figure 3).

Figure 3:



(A) Full Spectrum absorbance for each stock SPION dilution (black), as well as for each conjugated-SPION dilution.

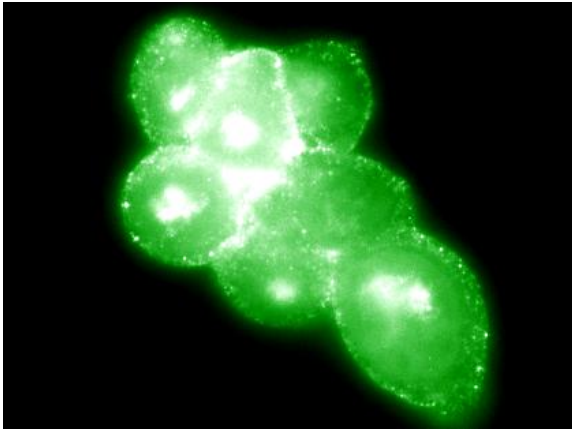
(B) Standard best fit of absorbances at 350 nm for stock SPION dilutions, used to determine (C) yield from each conjugation.

β3 Immunohistochemistry (IHC)

IHC was carried out to show the relative expression of αVβ3 integrin in cells. HUVEC, MDA-MB-231, and MDA-MB-435 cell lines were also included along with SK-OV-3 cells as a positive control, as well as to correlate the relative presence of αVβ3 with c(RGDfK) conjugated SPION activity. For this experiment, adherent cells were first lifted using EDTA, and suspended during incubations in order to view αVβ3 presence on all sides, including adherent portions of the cell surface. A polyclonal β3 antibody containing an RGD sequence was used to label cells. This staining was successful in all cell types, with the greatest overall presence of αVβ3 integrin shown in SK-OV-3 (Figure 4A) and MDA-MB-231 (Figure 4B) cell lines.

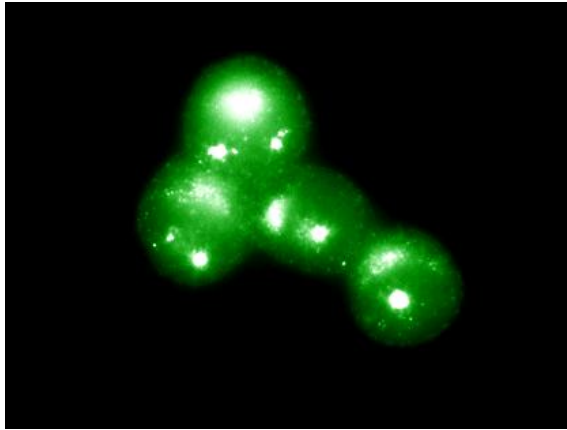
Figure 4:

A.



(A) $\beta 3$ - IHC for SK-OV-3 Cells 64x

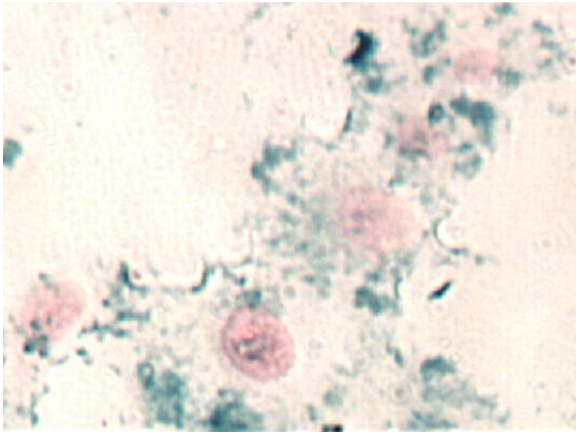
B.



(B) $\beta 3$ - IHC for MDA-MB-231 Cells 64x

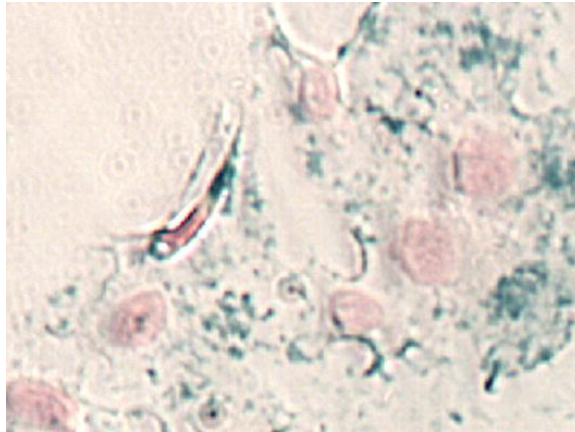
Figure 5:

A.



(A) SK-OV-3 cells 32x.
SPIONs covalently conjugated to c(RGDfK),
which selectively binds to $\alpha V\beta 3$.

B.



(B) SK-OV-3 Cells 32x.
SPIONs covalently conjugated to c(RADfK),
which does not bind $\alpha V\beta 3$ as a negative control.

Particles are visible in blue, and Nuclei in red following prussian blue histology. The lack of difference between the c(RGDfK) conjugated, and c(RADfK) conjugated control SPIONs suggests that only non-specific binding occurs.

c(RGDfK)(PEG-PEG))-SPION Incubation

Accounting for possible steric hindrance from particles being too closely associated with RGD peptide, SPIONs were conjugated with c(RGDfK)(PEG-PEG)) peptide. This analog contains two mini-PEG derivatives (8-amino-3,6-dioxaoctanoic acids) that act as spacers between the ligand and the particle surface to allow for more efficient binding^[20]. For this experiment, HUVEC, MDA-MB-231, and MDA-MB-435 cell lines were included along with SK-OV-3 cells to correlate the relative presence of $\alpha V\beta 3$ with functionalized SPION activity. Particle internalization was again generally minimal, with no observable difference between cell types or conjugates. This again suggests that only non-specific binding occurs for c(RGDfK)(PEG-PEG)) conjugated SPIONs.

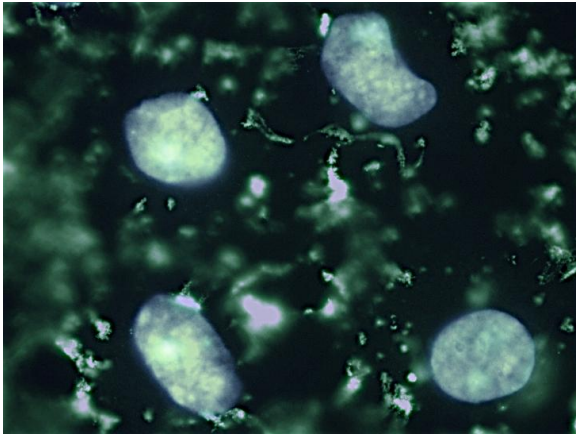
α VEGFR-2 Conjugated SPIONs

HUVECs, having the highest confirmed expression of VEGFR-2 from IHC, were used for particle incubations with α VEGFR-2 conjugated SPIONs, and with IgG conjugated SPIONs as a negative control. After incubations, cells were fixed, incubated with a blocking agent, and lastly incubated with secondary antibody to reveal

labeled particles attached at the cells surface. α VEGFR-2 conjugated SPIONs (Figure 5A) demonstrated effective functionalization, binding around the cell surface at high concentrations, while IgG conjugated SPIONs (Figure 5B) were only found minimally associated with cells.

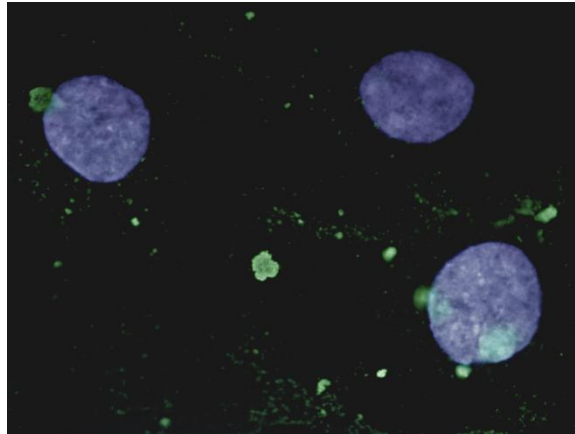
Figure 6:

A.



(A) HUVEC cells 64x.
 α VEGFR-2 Conjugated SPIONs demonstrated specific binding at high concentrations.

B.

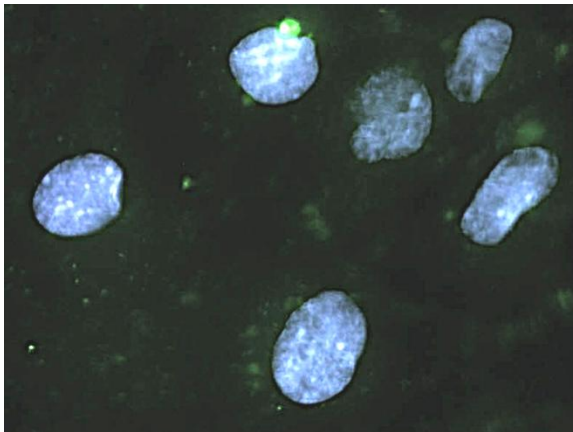


(B) HUVEC cells 64x.
IgG Conjugated SPIONs showed some association with the cell surface, representative of non-specific binding.

SPIONs are visible in green (2° AB - 488 nm), and nuclei in blue (DAPI - 358 nm).

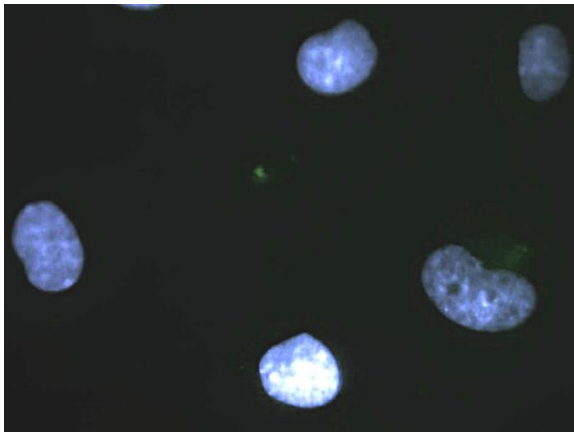
Figure 7:

A.



(A) HUVEC cells 64x.
 α VEGFR-2 Conjugated to PEG-Carboxyl SPIONs demonstrated specific binding. This overall binding was reduced however when compared to carboxyl-SPIONs conjugated to α VEGFR-2 (Figure 6A).

B.



(B) HUVEC cells 64x.
IgG Conjugated to PEG-Carboxyl SPIONs showed very minimal association with the cell surface, representative of a very low level of non-specific binding.

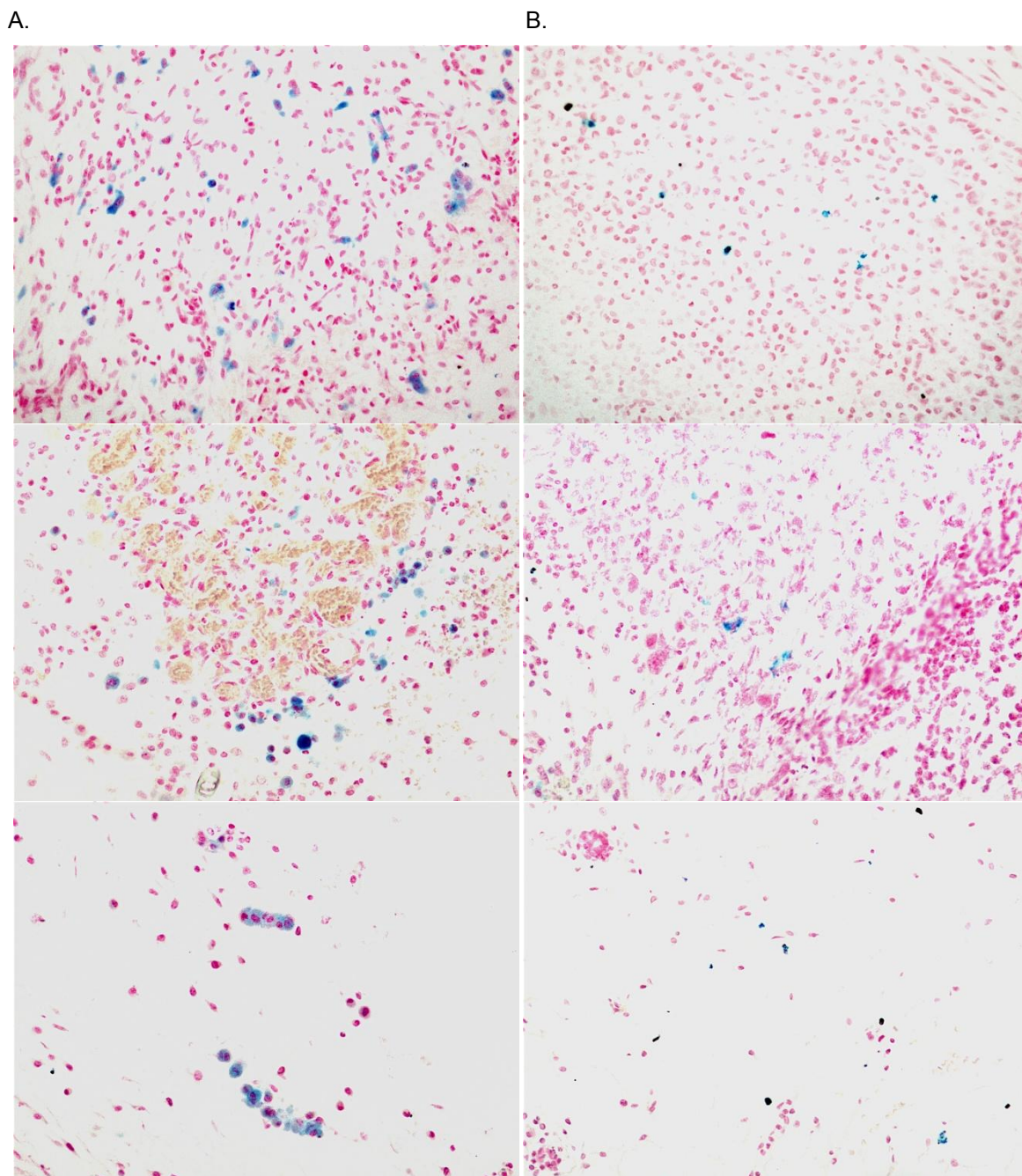
SPIONs are visible in green (2° AB - 488 nm), and nuclei in blue (DAPI - 358 nm).

Conjugated SPION Murine Tumor Delivery

When injected with carboxyl-SPIONs which were conjugated to α VEGFR-2, particles were apparently quickly cleared, with no tumor delivery observed. Carboxyl-SPIONs were then replaced by particles with a PEG-Carboxyl surface functionalization. The polymeric PEG coating acts to improve the stability of particles, and has been shown to increase the blood half-life of particles in vivo by up to 5 fold^[15]. These particles show

sustained stability in biological conditions, but also demonstrate reduced binding to HUVECs (Figure 7A) compared to VEGFR-2 conjugated particles without PEG (Figure 6A). However, the addition of PEG has the benefit of reducing non-specific binding of IgG-conjugated particles (the negative control condition) to HUVECs (comparing Figure 6B to Figure 7B). When injected alone, a small degree of α VEGFR-2-SPION localization at the tumor rim was observed (Figure 8B). Delivery was qualitatively increased when the particles were injected at 15 min following VDA treatment (Figure 8A). Tumor delivery was reduced however when α VEGFR-2-SPIONs were injected 30 min following VDA treatment.

Figure 8:

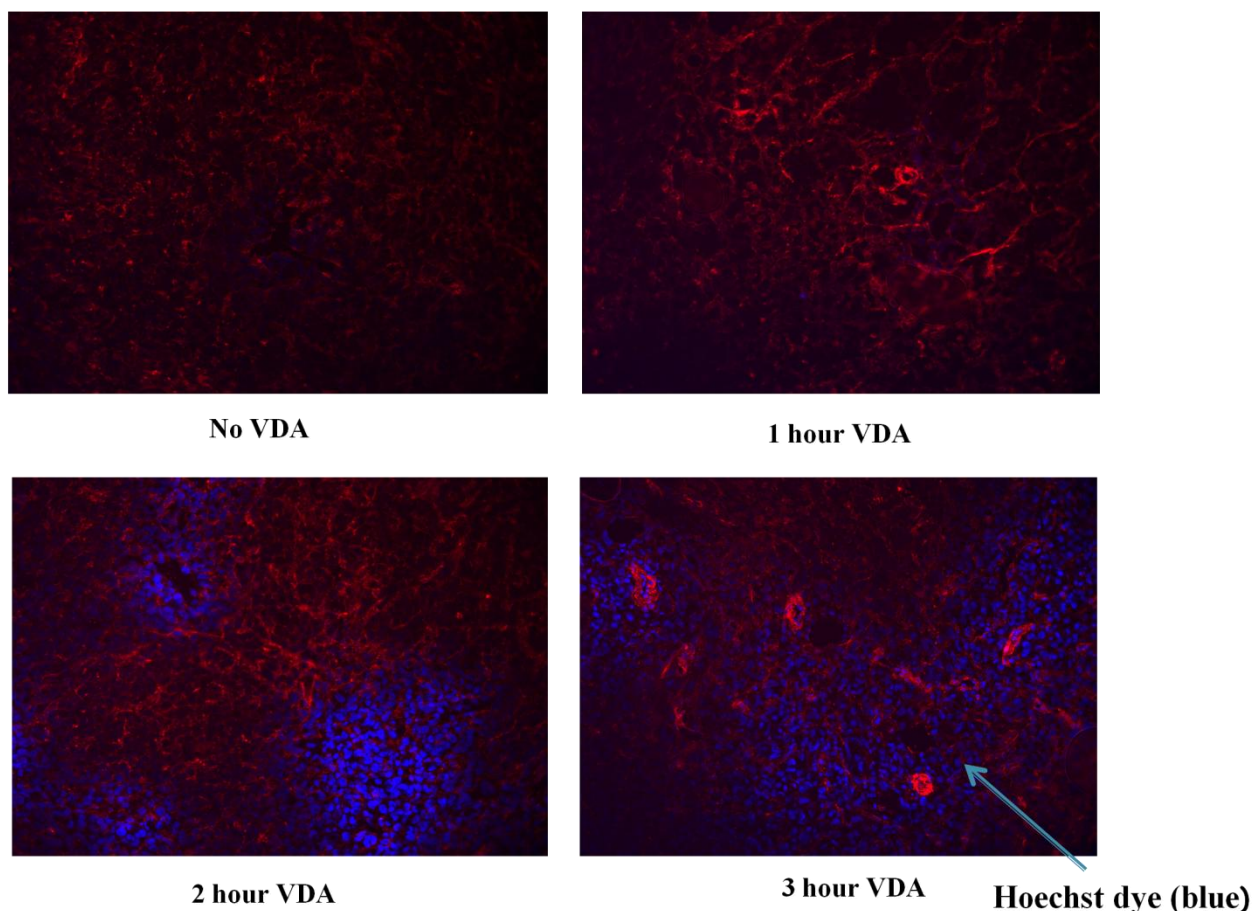


(A) Mouse tumor section at 20x. α VEGFR-2 conjugated SPIONs 15 min following VDA treatment show enhanced particle delivery to the tumor rim.

(B) Mouse tumor section at 20x. α VEGFR-2 conjugated SPIONs without VDA treatment show some particle delivery to the tumor rim when given alone.

Further changes in neovascular permeability in response to VDAs, which include the induction of endothelial apoptosis^[16], blood vessel rupture, and a boost of N_2O ^[17] are all reported to occur after about 12-24 h. We hypothesized that these late alterations in tumor physiology after VDA treatment may also be favorable to increasing SPION delivery. In the process of evaluating this hypothesis in vivo, we discovered that the tumor-bearing NOD/SCID mice were not surviving DMXAA pre-treatment for more than 6 hours. This was perplexing, given that non-tumor-bearing mice, used in our initial testing of the DMXAA dosing, showed no adverse effects. Given that our ultimate goal is to evaluate combination VDA/SPION treatment of tumors over a period of weeks, the poor long term survival after DMXAA administration was a critical issue to address. Further evaluation of the problem revealed that tumor-bearing mice (but not normal mice) were having an adverse reaction to the DMSO used to dissolve the poorly-soluble DMXAA into a volume that could be safely injected. Further research revealed that a 5% sodium bicarbonate buffer could be used to dissolve the drug in a reasonable volume, and the new bicarbonate formulation was well-tolerated by normal and tumor-bearing mice over many days.

Figure 9.

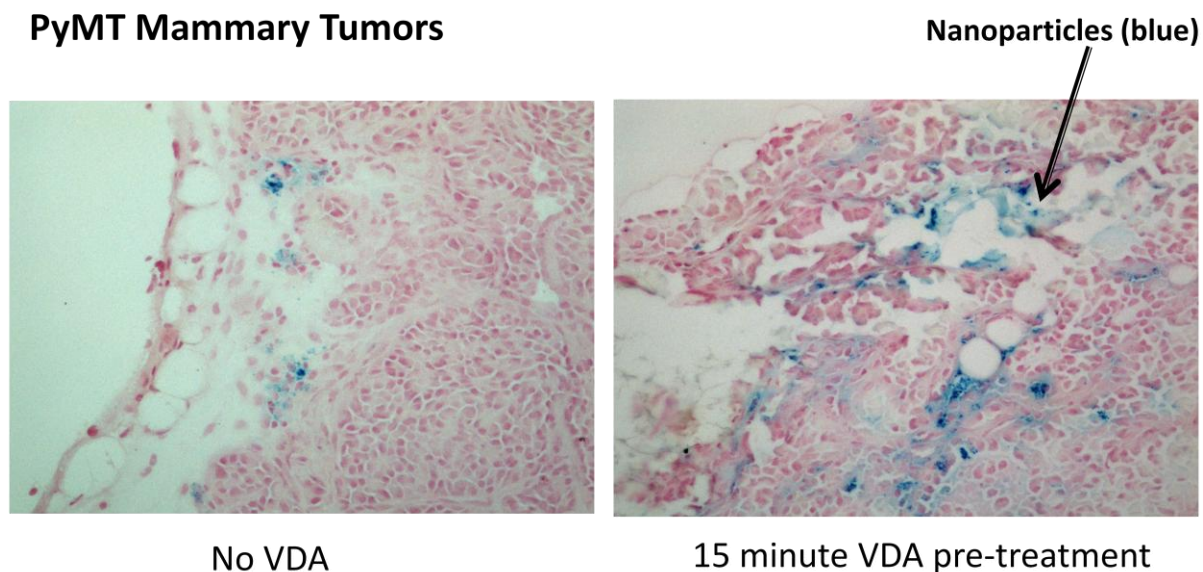


- The Hoechst dye (blue) is injected intravenously just prior to sacrificing the mouse and stains regions of the tumor that are well-perfused. Extravasation of dye from leaky tumor vessels may also contribute to the observed staining. F-actin in the cellular cytoskeleton is stained red by rhodamine phalloidin.
- Over a time course of three hours, VDA treatment resulted in increasing perfusion/permeability, with greater Hoechst staining observed over a wider area in the 2 to 3 hour post-VDA time period. The fluorescent images shown are sections of xenograft tumors in NOD SCID mice sacrificed at various time points following the injection of VDA.

With the new DMXAA formulation, we then performed a number of further experiments, including 1) verification (using Hoechst staining) of the drug's ability to alter perfusion/permeability in tumors (Figure 9 above) and 2) tests of whether longer VDA pre-treatments (20 hours) increase SPION delivery to the tumor rim (data not shown). Using Hoechst staining (delivered intravenously immediately prior to sacrificing the mice), we verified that the bicarbonate formulation of DMXAA produces an increase in deposition of the dye in tumor tissue following DMXAA administration. The increase in the volume of the tumor that stains blue after DMXAA treatment suggests that the VDA is having the desired effect of increasing perfusion/vascular permeability, which allows more dye to reach tumor tissue. Experiments performed using NOD/SCID mice with xenograft tumors to assess whether a longer period of VDA pre-treatment (20 hours) would be effective at increasing SPION delivery to tumors. These experiments revealed no difference between No VDA and 20 h VDA pre-treatment (data not shown).

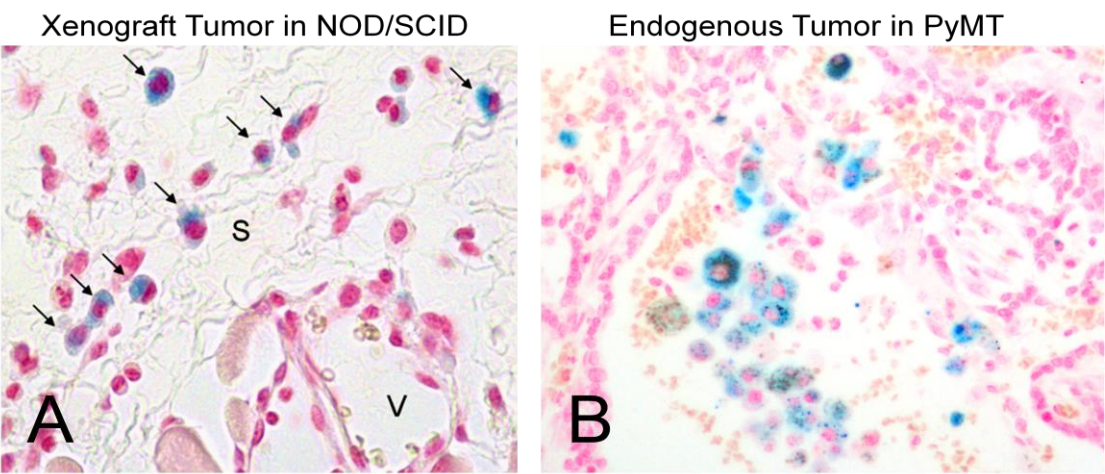
Based on Dr. Hathaway's recent experience with the PyMT tumor model (not originally proposed for use in this study), we felt that it would be worthwhile to test the DMXAA 15 minute pre-treatment combined with α VEGFR2-PEG-SPIONs in the PyMT model, because we hypothesized that the PyMT tumors would be better-vascularized. The PyMT model we used is a transgenic mouse (on a FVB background) that spontaneously and reliably develops mammary tumors at 10 weeks and metastases (primarily lung) at approximately 14 weeks. The tumors are therefore not xenografts but are instead malignant mouse mammary cells. Thus all components of the tumor environment (blood vessels, stroma, tumor) are formed from mouse cells. Unlike xenograft models, which require an immunocompromised mouse to avoid rejection of the tumor, the PyMT mouse model is an immune-competent mouse with a fully functioning immune system. Thus the PyMT tumor microenvironment also includes immune cell populations (such as tumor-associated macrophages) similar to those found in human breast tumors.

Figure 10:



Generally the vessel density in PyMT tumors is higher than that observed in xenografts, which often have relatively few main vessels feeding the tumor. Indeed, SPION delivery appears to be superior in PyMT mouse mammary tumors (relative to xenografts) based on our limited preliminary study. (See Figure 10 above.) Further, we observe more significant penetration of SPIONs phagocytosed by monocytes in the PyMT model. (See Figure 11 below.)

Figure 11:



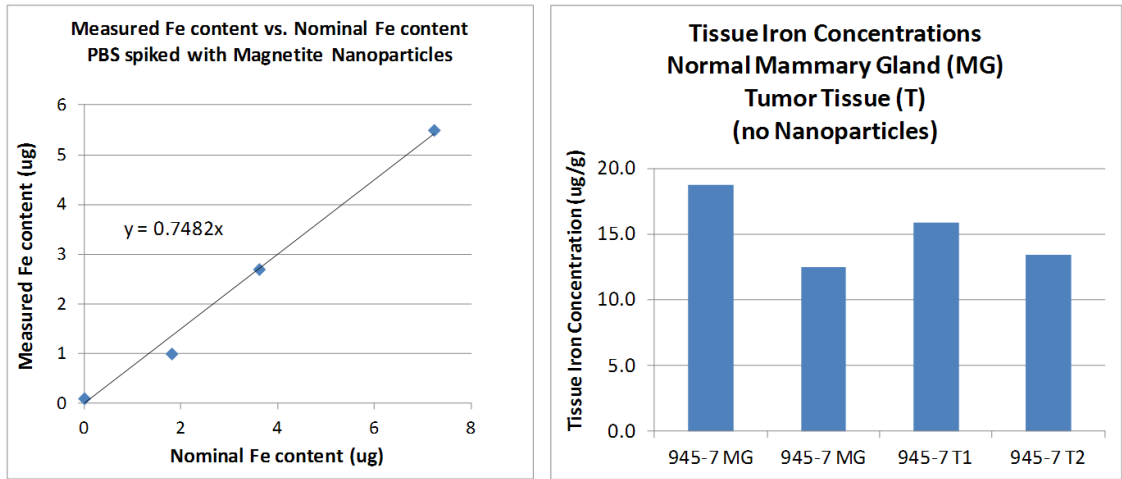
A: Micrograph of an MDA-MB-231 xenograft breast tumor in a NOD/SCID mouse (human tumor cells/mouse host). Prussian blue reveals *in vivo* SPION uptake by monocytes (black arrows) that have infiltrated the stroma (which is composed of mouse cells) 6 hrs. after i.v. injection of 15 nm SPIONs. Blue-stained monocytes were not observed in more the cellular areas of the tumor (human cells). S = stroma, V = vessel

B: Micrograph of an endogenous mammary tumor in a PyMT mouse (mouse tumor cells/mouse host). Prussian blue again reveals SPION uptake by monocytes that have begun to infiltrate more cellular regions of the tumor only 2 hrs. after i.v. injection of 15 nm VEGFR2-PEG SPIONs. Phagocytic tumor-infiltrating immune cells appear to be an important component of SPION delivery to mammary tumors in this immune-competent model.

Quantitation of SPIONs delivered In Vivo

As shown in Figure 12 below (left graph), we determined that inductively coupled plasma mass spectrometry (ICP-MS) of iron is sensitive enough to quantify the microgram quantities of iron that we expect to deliver to tumors in the form of iron-oxide nanoparticles. Unfortunately, further quantitative assessments of tumor tissue (which showed varying levels of SPION delivery by Prussian blue microscopy) revealed no clear trend in the iron content of the tumor tissue by ICP-MS.(data not shown) Further investigation revealed that the background endogenous iron levels in breast tumor tissue are of order 10-20 micrograms Fe per gram tissue (Figure 12, right graph), and the variation (several micrograms/g) is greater than the expected total iron content of SPIONs delivered to tumors. Thus the ICP-MS method is sensitive enough, but not specific enough, to quantify iron from SPIONs in tumor tissue. The issue of quantifying SPION delivery will need to be addressed in a future study.

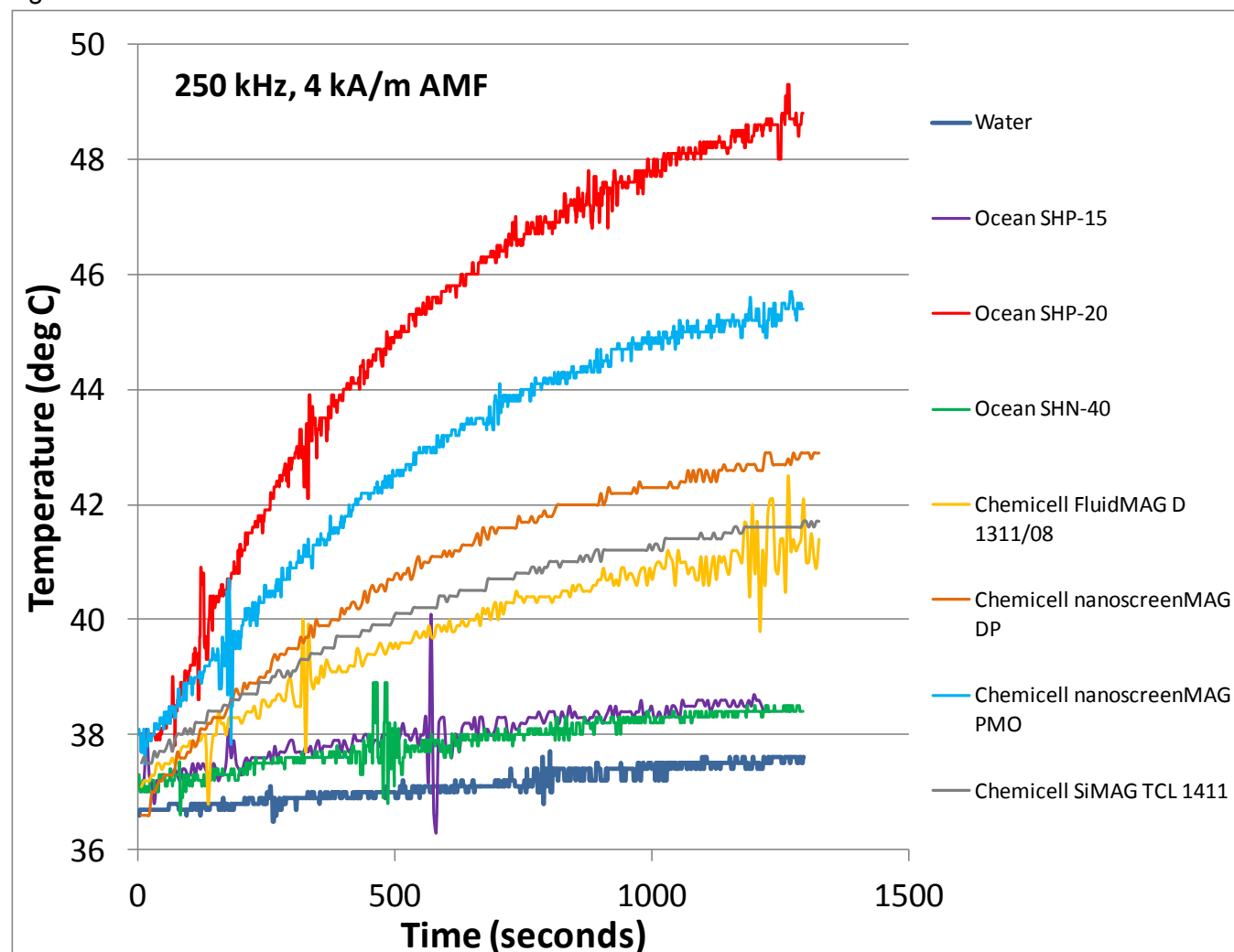
Figure 12:



SPION heating under Alternating Magnetic Field Conditions

In preparation for in vivo testing of hyperthermia therapy (Task 2), SPIONs in aqueous solution were exposed to a biocompatible alternating magnetic field (AMF), i.e. using a field strength and frequency safe for normal tissue. The sample chamber was maintained at a background temperature of 37 deg. C, suitable for future in vivo testing. A sample containing only water (no nanoparticles) showed a temperature rise <1 deg C after 20 minutes, which demonstrates that the AMF conditions are safe for normal tissues. Ocean SHP-20 SPIONs yielded the greatest heating capacity and will be used in future in vivo studies of hyperthermia therapy.

Figure 13:



Sample temperature (deg C) vs. Time (seconds) for various types of SPIONs in water. The AMF conditions (frequency = 250 kHz, field amplitude = 4 kA/m) are safe for normal tissue, but produce significant heating in the presence of Ocean SHP-20 SPIONs.

Discussion

When compared to unconjugated carboxyl functionalized SPIONs, c(RGDfK)-conjugated carboxyl SPIONs show greater colloidal stability at physiological pH and salinity, indicating a successful conjugation. In vitro, these SPION conjugates were, however, ineffective at targeting cell types shown by IHC to highly express the receptor for the RGD ligand ($\alpha v \beta 3$ integrin). This could be due to the misorientation of c(RGDfK) following the conjugation, steric hindrance from the overcrowding of peptide on the particle surface, or possibly due to the steric hindrance of ligand/receptor interaction from particles themselves. Attempts to reduce steric hindrance using a c(RGDfK) peptide with a PEG linker (to extend the distance between the RGD and the nanoparticle surface) were also unsuccessful.

When conjugated to α VEGFR-2 antibody, SPIONs demonstrated effective in vitro targeting of VEGFR-2 expressing human epithelial cells. The antibody clone chosen has also been shown to react with mouse VEGFR-2. While this model was effective for cell targeting under culture conditions, tumor models provide additional obstacles to overcome for SPION delivery. Initial injections of SPIONs in tumor bearing mice resulted in the apparently rapid clearance of particles (particles observed in liver, spleen, and to a small extent, lung), with no tumor delivery. In order to improve SPION circulation time for more effective tumor delivery, carboxyl-SPIONs were replaced by particles which were functionalized with both a PEG and carboxyl coating. The added stability of including PEG on the surface of α VEGFR-2-SPIONs coincided with a reduction in binding to HUVECs in vitro, but also a desirable reduction in non-specific binding of IgG-SPIONs to HUVECs. The reduced binding of α VEGFR-2-SPIONs to HUVECs is presumed to be due to a reduction of the conjugation efficiency of α VEGFR-2 to SPIONs, because the presence of PEG reduces the number of carboxyl sites on the particle surface. These particles did, however, demonstrate a modest level of delivery to the tumor rim when injected alone into mice (i.e. without the addition of VDA). Thus the addition of PEG appears to be beneficial for in vivo delivery of these particles.

The initial VDA response, which results in the alteration of the junctions between endothelial cells,^[13] appears to increase the delivery of α VEGFR-2-conjugated SPIONs to the tumor rim when the particles were injected 15 min after DMXAA. A lower level of delivery was observed from IgG-conjugated SPIONs under the same VDA conditions. Overall, the combination of VEGFR-2 targeting and 15 min. pre-administration of VDA appears to act synergistically to increase SPION delivery to the tumor rim. These results, which have been assessed qualitatively using Prussian blue histology could not be confirmed quantitatively (by iron mass spectrometry), due to the high endogenous iron concentration in breast tumor tissue.

Further changes in neovascular permeability in response to VDAs, which include the induction of endothelial apoptosis^[16], blood vessel rupture, and a boost of N_2O ^[17] are all reported to occur after about 12-24 h. These events could similarly enhance the delivery of SPIONs; however, our study comparing a 20 h pre-treatment by DMXAA compared to no DMXAA showed no enhancement of SPION delivery using the 20 h DMXAA treatment.

A limited study using an immunocompetent mouse mammary tumor model showed promising results. Transgenic PyMT-FVB mice spontaneously develop tumors in their mammary glands by 10 weeks of age. The advantages of this immunocompetent mouse tumor model include better vascularization of the growing tumor and a tumor microenvironment (including an immunological component, e.g. tumor-associated monocytes and macrophages) that better recapitulates human breast tumors. As we observed previously in a xenograft model (MDA-MB-231 tumors in NOD/SCID mice), there was a noticeable enhancement of SPION delivery to tumor tissue in PyMT mice using a 15 min DMXAA pre-treatment, compared to no DMXAA. Perhaps more importantly, we observed an overall increase in SPION delivery to tumors using the PyMT model. In other words, PyMT tumor-bearing mice, both with and without DMXAA pre-treatment, showed greater and more uniform SPION delivery to tumor tissue, relative to NOD/SCID mice with xenograft tumors under the same experimental conditions. Further, the participation of immune cells in delivering SPIONs to tumor tissue was observed to be more significant in the immunocompetent PyMT model.

The heating which can be achieved by exposing SPIONs to an AMF is shown to be linearly proportional to particle concentration^[6], indicating that effectiveness is directly proportional to delivery. Thus our demonstration that combining the targeted α VEGFR-2 conjugated SPIONs with VDA mediated vascular permeability increases particle delivery is an important first step in developing this therapy. We have further succeeded in identifying a more suitable mouse model (transgenic PyMT-FVB) for testing this therapy going forward. The fact that female PyMT mice develop both primary mammary tumors and lung metastases is an added advantage. Additionally, we have determined a superior formulation for administering the vascular disrupting agent DMXAA required for future longitudinal studies of this therapeutic method.

Problems Encountered

Task 1.

- The preparation of neovascular-targeted SPIONs proceeded more slowly than initially anticipated, but the initial problems with lack of neovascular binding specificity were eventually solved.
- SQUID magnetorelaxometry, although sufficiently sensitive to detect intratumorally injected SPIONs [23], has not been able to achieve the sensitivity required to monitor targeted SPION uptake in tumors after systemic i.v. delivery. We had hoped that the SPION concentrations after VDA therapy might be high enough to enable in vivo monitoring by SQUID magnetorelaxometry, but so far the concentration is too low. Thus, in vivo SQUID magnetorelaxometry was not pursued for these studies, and instead inductively-coupled plasma mass spectrometry (ICP-MS) of iron, which is a much more sensitive technique, is being used to quantitatively assess tumor iron content in fixed tissue samples.
- Although the sensitivity of ICP-MS was found to be adequate for quantifying iron in quantities of nanoparticles relevant to tumor delivery, the specificity of ICP-MS proved to be inadequate due to high endogenous iron levels in breast tumor tissue (in the absence of SPIONs).

Task 2.

- A problem with the long-term survival of mice receiving DMXAA (resulting in enlarged spleens, hemorrhage, and death) considerably slowed work on Task 2. The problem was eventually solved, which will enable the in vivo testing described in Aim 2, which requires long term survival after DMXAA administration, to be carried out in future studies.
- After solving the DMXAA toxicity problem, further studies in a NOD/SCID xenograft mouse model showed modest delivery of SPIONs to tumor using, but the SPION delivery was not great enough to warrant in vivo therapy studies. (The SPION concentration was high in isolated tumor regions, but overall was too low to produce SPION heating under alternating magnetic fields.) A limited study of SPION delivery to a PyMT endogenous mouse mammary tumor model showed a greater overall distribution of SPIONs in tumor tissue. While the latter findings are promising, they occurred too late in the project period to pursue hyperthermia studies under this award.

Key Research Accomplishments

- production of functional α VEGFR-2-conjugated PEG-coated iron oxide nanoparticles, with binding specificity verified in vitro
- synergistic enhancement of SPION delivery when α VEGFR-2-conjugated PEG-coated SPIONs are administered following 15 min. DMXAA pre-treatment, demonstrated by:
 - greater in vivo delivery of α VEGFR-2-conjugated PEG-coated SPIONs relative to α VEGFR-2-conjugated SPIONs (no PEG)
 - greater in vivo delivery of α VEGFR-2-conjugated PEG-coated SPIONs when administered 15 min. after VDA injection, relative to α VEGFR-2-conjugated PEG-coated SPIONs alone (no DMXAA)
 - greater in vivo delivery of α VEGFR-2-conjugated PEG-coated SPIONs administered 15 min. after DMXAA injection, relative to IgG-conjugated PEG-coated SPIONs or PEG-coated SPIONs (no antibody)

Reportable Outcomes

- Eric Joseph, an undergraduate Biochemistry Honors student, presented the work he did on this project at Biochemistry Research Day (April 28, 2012, University of New Mexico). Upon graduation in May 2012, Eric received a Bachelors of Science with Magna Cum Laude Honors in Biochemistry and

received the Lofffield Research Award, the most prestigious student research prize awarded by our department.

- Based on his experience working on this project, Eric Joseph, B.S., was hired in June 2012 as a Research Technician II at the Oregon Health Sciences University (from a pool of more than 100 applicants). This fall, Eric plans to apply to the Ph.D. program at OHSU. Eric has indicated that he would not have considered a career as a scientific researcher prior to working on this project.
- Training opportunities were also provided to three additional students Shayna Kim (undergraduate), Lauren Marek (undergraduate), and Jaclyn Murton (master's student), who all participated in various aspects of this work. Lauren and Jaclyn both presented their results in posters at Biochemistry Research Day (April 20, 2013, University of New Mexico).
- Natalie Adolphi (PI) applied for and received a UNM Cancer Center pilot award (\$5k) to pursue radioimaging of monocyte infiltration of tumors, based in part on micrographs showing infiltration of monocytes that had ingested SPIONs in vivo, obtained during these studies. Additionally, Helen Hathaway (Co-I) applied for and received UNM Research Allocation committee funds (\$25k) to study delivery of SPIONs to tumors using monocyte adoptive transfer. Both of these additional awards are supporting the master's thesis work of Jaclyn Murton.
- A provisional patent 2011-044 was filed December 20, 2012; however, the provisional has so far not been converted to a utility patent application.

Conclusions

Task 1.

- Significant progress on Task 1 has been achieved, with current in vivo results suggesting synergistic enhancement of SPION delivery to the tumor rim when α VEGFR-2 targeting of PEG-coated particles and 15 min pre-administration of DMXAA are employed in both a xenograft tumor model (immune compromised mouse) and an endogenous tumor model (immune competent mouse). Thus the combination of targeting the neovasculature and increasing vascular permeability through the action of the VDA appears to be an effective SPION delivery strategy.
- We note that the conjugation chemistry that proved successful was covalent coupling of a primary amine on the antibody to a carboxyl on the SPIONs activated by EDC/Sulfo-NHS. Strategies that were attempted but abandoned included SATA coupling of RGD to SPIONs (originally proposed in Task 1), carboxyl/EDC coupling of RGD to SPIONs, carboxyl/EDC coupling of RGD with a PEG spacer to SPIONs – these strategies were deemed unsuccessful because they did not result in specific binding of SPIONs to appropriate cell types in vitro. The successful conjugation resulted in colloiddally-stable particles that showed specific binding to VEGFR-2 expressing cells in vitro.
- Comparison of SPION delivery to xenograft tumors in an immune-compromised mouse model (NOD/SCID) vs. endogenous tumors in an immune-competent mouse model (PyMT) reveals that SPION delivery to tumor tissue is greater in the PyMT tumor model, suggesting that this model may be more suitable for future development and testing of the proposed synergistic VDA/SPION therapy.

Task 2.

- Preliminary in vitro testing of the ability of the SPIONs to generate heat in the presence of an alternating magnetic field has been successful, indicating an optimum nanoparticle diameter of 20 nm.

- An improved formulation of the DMXAA, suitable for in vivo therapy studies, was developed and tested.
- In vivo testing of hyperthermia therapy in mice receiving targeted SPIONs after DMXAA pre-treatment was not attempted, because satisfactory SPION delivery (high enough to warrant longitudinal in vivo hyperthermia trials) was only achieved at the very end of the project period.

References

1. Gaya AM, Rustin GJ. Vascular disrupting agents: a new class of drug in cancer therapy. *Clin Oncol (R Coll Radiol)*. 2005 Jun;17(4):277-90. Review. PubMed PMID: 15997924.
2. Eiki Ichihara, Katsuyuki Kiura, and Mitsune Tanimoto. Targeting angiogenesis in cancer therapy. *Acta Med Okayama*. 2011 Dec;65(6):353-62.
3. Hsu AR, Veeravagu A, Cai W, Hou LC, Tse V, Chen X. Integrin alpha v beta 3 antagonists for anti-angiogenic cancer treatment. *Recent Pat Anticancer Drug Discov*. 2007 Jun;2(2):143-58.
4. Ylä-Herttuala S, Rissanen TT, Vajanto I, Hartikainen J. Vascular Endothelial Growth Factors: Biology and Current Status of Clinical Applications in Cardiovascular Medicine. *Journal of the American College of Cardiology*, March 2007; 49 (10, 13): 1015-1026.
5. Rosensweig RE. Heating magnetic fluid with alternating magnetic field. *J Magn Magn Mater*. 2002;252:370–4.
6. Kenya Murase, Junko Oonoki, Hiroshige Takata, Ruixiao Song, Anggia Angraini, Prapan Ausanai, Taro Matsushita. Simulation and experimental studies on magnetic hyperthermia with use of superparamagnetic iron oxide nanoparticles. *Radiol Phys Technol* (2011) 4:194–202 DOI 10.1007/s12194-011-0123-4.
7. I Marcos-Campos, L Asin, T E Torres, C Marquina, A Tres, M R Ibarra, and G F Goya. Cell death induced by the application of alternating magnetic fields to nanoparticle-loaded dendritic cells. *Nanotechnology* 22 (2011) 205101 (13pp) doi:10.1088/0957-4484/22/20/205101.
8. Y Ueda, T Yamagishi, K Smata, N Hirayama, Y Aozuka, M Tanaka, S Nakaike, and I Saike. Antitumor Effects of Synthetic VEGF-receptor Binding Antagonist, VGA1155. *Anticancer Research* 25: 3973-3978 (2005).
9. C.C. Kumar. Integrin alpha v beta 3 as a therapeutic target for blocking tumor-induced angiogenesis. *Curr Drug Targets*, 4 (2003), pp. 123–131.
10. Stephen D Robinson, Kairbaan M Hodivala-Dilke, The role of β 3-integrins in tumor angiogenesis: context is everything, *Current Opinion in Cell Biology*, Volume 23, Issue 5, October 2011, Pages 630-637.
11. Garanger E, Boturyn D, Dumy P. Tumor targeting with RGD peptide ligands-design of new molecular conjugates for imaging and therapy of cancers. *Anticancer Agents Med Chem*. 2007 Sep;7(5):552-8.
12. Lyshchik A, Fleischer AC, Huamani J, Hallahan DE, Brissova M, Gore JC. Molecular Imaging of Vascular Endothelial Growth Factor Receptor 2 Expression Using Targeted Contrast-Enhanced High-Frequency Ultrasonography. *J Ultrasound Med*, 2007; 26: 1575–1586.
13. Baguley. Antivascular therapy of cancer: DMXAA, *The Lancet Oncology*, Volume 4, Issue 3, March 2003, Pages 141-148, ISSN 1470-2045, 10.1016/S1470-2045(03)01018-0.
14. Smith GP, Calveley SB, Smith MJ, et al. Flavone acetic acid (NSC 347512) induces haemorrhagic necrosis of mouse colon 26 and 38 tumours. *Eur J Cancer Clin Oncol* 1987; 23: 1209–12.

15. E. Allard-Vannier, S. Cohen-Jonathan, J. Gautier, K. Hervé-Aubert, E. Munnier, M. Soucé, P. Legras, C. Passirani, I. Chourpa, Pegylated magnetic nanocarriers for doxorubicin delivery: A quantitative determination of stealthiness in vitro and in vivo, *European Journal of Pharmaceutics and Biopharmaceutics*, Available online 10 April 2012, ISSN 0939-6411, 10.1016/j.ejpb.2012.04.002.
16. Robaye B, Mosselmans R, Fiers W, et al. Tumor necrosis factor induces apoptosis (programmed cell death) in normal endothelial cells in vitro. *Am J Pathol* 1991; 138: 447–53.
17. Lindy L. Thomsen, Lai-Ming Ching, Wayne R. Joseph, Bruce C. Baguley, John B. Gavin, Nitric oxide production in endotoxin-resistant C3H/HeJ mice stimulated with flavone-8-acetic acid and xanthenone-4-acetic acid analogues, *Biochemical Pharmacology*, Volume 43, Issue 11, 9 June 1992, Pages 2401-2406, ISSN 0006-2952, 10.1016/0006-2952(92)90319-E.
18. Davis ME, Chen Z, Shin DM. Nanoparticle Therapeutics: An Emerging Treatment Modality for Cancer. *Nature Reviews Drug Discovery*, September 2008; 7: 771-782.
19. Xie J, Chen K, Lee HY, Xu C, Hsu AR, Peng S, Chen X, Sun S. Ultrasmall c(RGDyK)-Coated Fe₃O₄ Nanoparticles and Their Specific Targeting to Integrin $\alpha\beta 3$ -Rich Tumor Cells. *Journal of the American Chemical Society*, 2008; 130 (24): 7542-7543.
20. P. Holig, M. Bach, T. Volkel, T. Nahde, S. Hoffmann, R. Muller, R.E. Kontermann. Novel RGD lipopeptides for the targeting of liposomes to integrin-expressing endothelial and melanoma cells. *Protein Eng. Des. Sel.*, 17 (2004), pp. 433–441.
21. R.M. Izatt, G.D. Watt, H.C. Bartholomew, J.J. Christensen. A calorimetric study of Prussian Blue and Turnbull's Blue formation. *Inorg. Chem.*, 9 (1970), pp. 2019–2021.
22. Zhao L, Baguley BC, Kestell P, et al. The antitumour activity of 5,6-dimethylxanthenone-4-acetic acid (DMXAA) in TNF receptor-1 knockout mice. *Br J Cancer* 2002; 87: 465–70.
23. Adolphi NL, Butler KS, Lovato DM, Tessier TE, Trujillo JE, Hathaway HJ, Fegan DL, Monson TC, Stevens TE, Huber DL, Ramu J, Milne ML, Altobelli SA, Bryant HC, Larson RS, Flynn ER. Imaging of Her2-targeted magnetic nanoparticles for breast cancer detection: comparison of SQUID-detected magnetic relaxometry and MRI. *Contrast Media Mol Imaging*. 2012 May-Jun;7(3):308-19. doi: 10.1002/cmml.499. PubMed PMID: 22539401.
24. McPhail LD, Chung YL, Madhu B, Clark S, Griffiths JR, Kelland LR, Robinson SP. Tumor dose response to the vascular disrupting agent, 5,6-dimethylxanthenone-4-acetic acid, using in vivo magnetic resonance spectroscopy. *Clin Cancer Res*. 2005 May 15;11(10):3705-13. PubMed PMID: 15897567.
25. Woon ST, Zwain S, Schooltink MA, Newth AL, Baguley BC, Ching LM. NF-kappa B activation in vivo in both host and tumour cells by the antivascular agent 5,6-dimethylxanthenone-4-acetic acid (DMXAA). *Eur Cancer*. 2003 May;39(8):1176-83. PubMed PMID: 12736120.
26. Ching LM, Cao Z, Kieda C, Zwain S, Jameson MB, Baguley BC. Induction of endothelial cell apoptosis by the antivascular agent 5,6-Dimethylxanthenone-4-acetic acid. *Br J Cancer*. 2002 Jun 17;86(12):1937-42. PubMed PMID: 12085190; PubMed Central PMCID: PMC2375421.
27. Vincent P, Roberts B, Elliott W, Leopold W. Chemotherapy with DMXAA (5,6-dimethylxanthenone-4-acetic acid) in combination with CI-1010 (1H-imidazole-1-ethanol, α -[[(2-bromoethyl)amino]methyl]-2-nitro-, mono-hydrobromide (R isomer)) against advanced stage murine colon carcinoma 26. *Oncol Rep*. 1997 Jan-Feb;4(1):143-7. PubMed PMID: 21590030.
28. Seshadri M, Spornyak JA, Maiery PG, Cheney RT, Mazurchuk R, Bellnier DA. Visualizing the acute effects of vascular-targeted therapy in vivo using intravital microscopy and magnetic resonance imaging: correlation with endothelial apoptosis, cytokine induction, and treatment outcome. *Neoplasia*. 2007 Feb;9(2):128-35. PubMed PMID: 17356709; PubMed Central PMCID: PMC1813934.